

# Mouse Keratin 4 Is Necessary for Internal Epithelial Integrity\*

(Received for publication, April 9, 1998, and in revised form, June 16, 1998)

Seth L. Ness<sup>‡§</sup>, Winfried Edelmann<sup>‡</sup>, Timothy D. Jenkins<sup>¶</sup>, Wolfgang Liedtke<sup>\*\*‡‡</sup>,  
Anil K. Rustgi<sup>¶§¶</sup>, and Raju Kucherlapati<sup>‡¶¶</sup>

From the <sup>‡</sup>Department of Molecular Genetics, Albert Einstein College of Medicine, Bronx, New York 10461, the <sup>¶</sup>Gastrointestinal Unit and the <sup>§§</sup>Hematology-Oncology Unit, Massachusetts General Hospital, Harvard Medical School, Boston, Massachusetts 02114, and the <sup>\*\*</sup>Department of Pathology/Division of Neuropathology, Albert Einstein College of Medicine, Bronx, New York 10461 and <sup>‡‡</sup>Howard Hughes Medical Institute, The Rockefeller University, New York, New York 10023

**Keratins are intermediate filaments of epithelial cells. Mutations in keratin genes expressed in skin lead to human disorders, including epidermolysis bullosa simplex and epidermolytic hyperkeratosis. We examined the role of keratin 4 (K4) in maintaining the integrity of internal epithelial linings by using gene targeting to generate mice containing a null mutation in the epithelial K4 gene. Homozygous mice that do not express K4 develop a spectrum of phenotypes that affect several organs which express K4 including the esophagus, tongue, and cornea. The cellular phenotypes include basal hyperplasia, lack of maturation, hyperkeratosis, atypical nuclei, perinuclear clearing, and cell degeneration. These results are consistent with the notion that K4 is required for internal epithelial cell integrity. As mutations in K4 in humans lead to a disorder called white sponge nevus, the K4-deficient mice may serve as models for white sponge nevus and for understanding the role of K4 in cellular proliferation and differentiation.**

The 10-nm intermediate filaments, along with actin and tubulin, form the cytoskeleton of cells in higher eukaryotes. Keratins are the intermediate filaments of epithelial cells. A large number of mammalian keratins have been identified and, based upon their biochemical properties, have been divided into two groups. The type I keratins, designated K9–K20,<sup>1</sup> are acidic, have molecular masses in the range of 40,000–63,000, and are clustered on human chromosome 17 and mouse chro-

mosome 11(1). The type II keratins, designated K1–K8, are basic, have molecular masses in the range of 53,000–67,000, and are clustered on human chromosome 12 and mouse chromosome 15(1). The hair keratins also fall into these two groups, and their genes are most likely interspersed with those of the epithelial keratins (2). The keratin proteins have an  $\alpha$ -helical structure and form heterodimers with one member from each group. Higher order structures of the keratin heterodimers constitute the intermediate filaments (1, 3).

Specific members of the type I and type II keratins are found to be characteristically associated with each other in different cell and tissue types. Simple epithelia, such as the gut, express predominantly K8 and K18. Stratified squamous epithelia express mainly K5 and K14 in their basal layers, while their suprabasal layers express K1 and K10 in skin and K4 and K13 in some internal epithelia, such as the esophagus (4).

Although epithelial cells in culture can survive in the complete absence of a keratin network (5), there is a significant amount of evidence that keratins play critical roles in the maintenance of cell integrity *in vivo*. Evidence in support of this view was obtained from the study of several human genetic disorders. One of the first disorders that was molecularly characterized was epidermolysis bullosa simplex (EBS) (OMIM 131760, 131900, and 131800). This disorder, usually inherited in an autosomal dominant fashion, is characterized by the lysis of the basal cells in the epidermis and the formation of skin blisters following mild trauma. The dominant form of EBS was shown to be the result of missense mutations in either the K5 or K14 genes (6–8). Autosomal recessive forms of EBS result from homozygous null mutations in the same genes (9, 10). Another skin disorder, epidermolytic hyperkeratosis (OMIM 113800), is characterized by blistering in the suprabasal layer and is the result of mutations in K1 or K10 (11–13).

To understand the role of keratins and the phenotypic manifestations of mutations in keratin genes expressed in internal epithelia, we generated mice with a null mutation in K4. We report that mice that are homozygous for the null mutation exhibit a spectrum of phenotypes in several organs including esophagus, tongue, and the cornea. These results suggest that K4 is required for the maintenance of internal epithelial cell integrity. It has recently been shown that the human disorder white sponge nevus (WSN, OMIM 193900) is the result of mutations of either K4 or K13 (14, 15). Although there are some differences in the spectrum of phenotypic manifestations in WSN patients and mice lacking the K4 protein, the mice could serve as genetic models for this disorder and may help us understand the pathophysiology resulting from the absence of K4 and the role of K4 in squamous epithelial cell differentiation. Based on the similarities between the K4-deficient mice and another human disease, hereditary benign intraepithelial

\* This work was supported in part by American Cancer Society Grant CN-132, National Institutes of Health Grant DK40561, Center Grant CA 13330 to Albert Einstein College of Medicine, and the Human Genetics Program at Albert Einstein College of Medicine. The costs of publication of this article were defrayed in part by the payment of page charges. This article must therefore be hereby marked "advertisement" in accordance with 18 U.S.C. Section 1734 solely to indicate this fact.

§ Supported by National Institutes of Health Training Grant T32GM07288.

¶ Supported by a Glaxo-Wellcome Institute for Digestive Health award and by National Institutes of Health Training Grant NIHT2DK07191D21.

¶¶ Supported by National Institutes of Health Grants DK 53377 and 1P01 DE 12467-01A1.

¶¶¶ To whom correspondence should be addressed: Dept. of Molecular Genetics, Albert Einstein College of Medicine, 1300 Morris Park Ave., Bronx, NY 10461. Tel.: 718-430-2069; Fax: 718-430-8776; E-mail: kucherla@aecom.yu.edu.

<sup>1</sup> The abbreviations used are: K, keratin; bp, base pair(s); kb, kilobase pair(s); PCNA, proliferating cell nuclear antigen; PCR, polymerase chain reaction; RT, reverse transcriptase; PAGE, polyacrylamide gel electrophoresis; WT, wild-type; EBS, epidermolysis bullosa simplex; WSN, white sponge nevus; TBS, Tris-buffered saline; TBS-T, Tris-buffered saline with Tween 20; MOPS, 4-morpholinepropanesulfonic acid.

dykeratosis (OMIM 127600), we suggest that mutations in K4 or K13 may also cause this disorder.

#### EXPERIMENTAL PROCEDURES

##### Screening of $\lambda$ 129 Library

To recover a full genomic clone of mouse keratin 4, a mouse genomic library (129/Ola, gift from Dr. O. Smithies, University of North Carolina, Chapel Hill, NC) was screened. The library was made with phage  $\lambda$  charon 35 digested with *Bam*HI and mouse genomic DNA digested with *Sst*I. It was plated on 20 plates with about 50,000 plaques/plate for a total of 1 million. The library represents 5 genomic equivalents and has an average insert size of 15 kb. The library was screened with a K4 insert from pMK1. The PCR-derived clone, pMK1, was digested with *Fok*I, which released an insert of around 490 bp containing almost all of intron 3 and only 6 bp of exon 4. A set of 20 filters were hybridized with the probe according to the method of Maniatis (16). Twenty positive plaques were picked. Seven of these were plaque-purified through two further rounds of plating and hybridization. Phage transformation, growth, and DNA extraction was performed by the method of Maniatis (16). Sequencing, restriction enzyme analysis, and Southern blot hybridization were used to identify a phage (designated clone 3) as an ideal substrate for construction of the targeting vector.

##### Generation of K4-deficient Mice

The 9.5-kb *Sac*I subclone of clone 3 in PC-DNA II, designated pMK4-4, contained the complete K4 gene, as determined by sequencing and restriction enzyme analysis, with the protein start site 484 bp into the clone. This fragment contains a unique *Xma*I site at bp 519, 12 amino acids into the protein. A 1.7-kb fragment containing the PGK-Neo cassette was inserted into this site in the reverse orientation. Additionally, for negative selection, a 1.8-kb thymidine kinase cassette was inserted into a unique *Xho*I site in the PC-DNA II polycloning region.

The targeting construct was linearized at the unique *Not*I site prior to transfection. Twenty-five micrograms of vector was transfected into  $5 \times 10^7$  WW6 ES cells using a Bio-Rad Gene Pulser set at 250 V and 500 microfarads. Transfected cells were transferred onto 20 10-cm feeder plates containing mitomycin-treated, neomycin-resistant embryonic fibroblasts and 9 ml of ES medium prepared according to Wurst and Joyner (17) except that the only serum was fetal calf, supplemented with leukemia inhibitory factor (Life Technologies, Inc.) at 1000 units/ml. Twenty-four hours after transfection the neomycin analog G418 (Life Technologies, Inc.) was added to the medium to a final concentration of 100  $\mu$ g/ml. Thirty-six hours after transfection, ganciclovir (GANC, Syntex, Palo Alto, CA) was added to a final concentration of 2  $\mu$ M. Drug selection was continued for 14 days or until discrete colonies were visible.

Colonies resistant to G418 and GANC were isolated and expanded in 24-well plates. Half of the cells from each well were frozen at  $-70^\circ\text{C}$ , and the other half were grown till confluence. Genomic DNA was prepared *in situ* by lysis and precipitation according to the method of Laird (18).

Screening for clones that were the result of gene targeting was performed using PCR. Primer set RK 825 5'-CCAATTTATGAGTCCCTGGGCT-3', corresponding to genomic DNA outside the targeting vector, and RK 482, 5'-TGGAAGGATTGGAGCTACGG-3', corresponding to neomycin sequences, amplified a unique 900-bp fragment from cells that had undergone a homologous recombination event.

ES cells from clones that were the result of gene targeting were injected into C57BL/6 recipient blastocysts and transferred to CD-1 pseudopregnant females. Genotyping was performed using PCR with a set of three primers. They were: RK 21649, 5'-CTGACAGCTTGC-CAAGCTCCCATC-3', RK 21652, 5'-TGCCGAAGCCCCAGAAGAGC-3', and RK 21651, 5'-AGGGCCAGCTCATTCTCCACTCA-3'. The primer set RK 21649 and RK 21652 yields a 727-bp product from the modified locus, and the set RK 21649 and RK 21651 yields an 830-bp product from the normal locus. Thus, wild-type mice will give one band of 727 bp, heterozygotes will give two bands of 727 and 830 bp, and homozygotes will give one band of 830 bp. Annealing was at  $66^\circ\text{C}$ .

##### PCR

PCR was performed in the Perkin-Elmer DNA thermal cycler or MJ-PTC100 programmable thermal controller (MJ Research Inc.). Reactions were typically performed using the following conditions: 0.2  $\mu$ M each primer, 0.2 mM dNTPs, 10 mM Tris-HCl, 50 mM KCl, 0.5–2.0 mM  $\text{MgCl}_2$ , 1–4 units of *Taq*. A total of 25–35 cycles were performed ( $94^\circ\text{C}$  for 20–120 s,  $50$ – $68^\circ\text{C}$  for 20–120 s, and  $72^\circ\text{C}$  for 45–240 s). Prior to

cycling, the template was melted at  $94^\circ\text{C}$  for 2 min, and, after cycling, an additional extension of 10 min was carried out at  $72^\circ\text{C}$ . PCR products were run on  $1 \times$  TBE gels of 1.0% agarose.

The primers used in the degenerate PCR were as follows: RK567, 5'-GAGAATGA(G/A)TTTGT(G/C)(G/C)TC(C/A)T-3', and RK568, 5'-CC(T/G)GAGGAAGTTGATCTC(A/G)T-3', at an annealing temperature of  $50^\circ\text{C}$ .

##### RNA Analysis

**Northern Blots**—Total RNA was extracted from fresh tissues using the TRIzol reagent (Life Technologies, Inc.) according to manufacturer's instructions. RNA was fractionated on 1% agarose gels prepared with  $10 \times$  MOPS buffer (200 mM MOPS, pH 7.4, 10 mM EDTA, pH 7.4, and 80 mM NaAC, pH 7.0) and 12.5% formaldehyde. Running buffer was  $1 \times$  MOPS. A total of 5–10  $\mu$ g of RNA was run per lane in three volumes of  $1.33 \times$  MOPS loading buffer (674  $\mu$ l of formamide, 216  $\mu$ l of formaldehyde, 30  $\mu$ l of 1 M MOPS, 3  $\mu$ l of 0.5 M EDTA, 10  $\mu$ l of 10% SDS, 10  $\mu$ l of 1% bromophenol blue/1% xylene cyanol mix, 57  $\mu$ l of glycerol, 2.5  $\mu$ l of ethidium bromide stock). Sample was heated for 3 min at  $65^\circ\text{C}$  and the gel was run overnight at 40 V. The RNA was transferred to Biotrans nylon membranes (ICN) using capillary transfer. For large probes, prehybridization and hybridizations were carried out in 0.25 M  $\text{Na}_2\text{HPO}_4$ , pH 7.2, and 7% SDS at  $65^\circ\text{C}$ . Blots were first washed at  $2 \times$  SSC, 0.1% SDS at room temperature. The final washes were performed at different stringencies, which varied from  $0.2 \times$  SSC, 0.1% SDS at  $42^\circ\text{C}$  to  $0.1 \times$  SSC, 0.1% SDS at  $65^\circ\text{C}$ . Blots were exposed to x-ray film (Amersham Pharmacia Biotech or Kodak) for 1–14 days.

**RT-PCR**—Total RNA was treated with 1 unit of DNase (Promega) and 0.2 units of RNasin per  $\mu$ g of RNA at  $37^\circ\text{C}$  for 1 h. The reverse transcriptase reaction was carried out with 20 units of avian myeloblastosis virus reverse transcriptase in a 20- $\mu$ l volume at  $1 \times$  PCR buffer (50 mM Tris, pH 8.4, 50 mM KCl), 2 mM  $\text{MgCl}_2$ , 100 ng of random hexanucleotides (Amersham Pharmacia Biotech), 10 units of RNasin, and dNTPs at 1 mM each per  $\mu$ g of total RNA. Annealing for 10 min at  $23^\circ\text{C}$  was followed by synthesis at  $42^\circ\text{C}$  for 1 h, followed by an incubation at  $94^\circ\text{C}$  for 10 min to inactivate the enzyme. The entire RT reaction was used in a PCR reaction of 100- $\mu$ l volume at conditions appropriate for the desired primers. A reaction without reverse transcriptase was used as a control for genomic DNA contamination. PCR products were analyzed on 1.0% agarose gels.

The primer pairs used were as follows: RK22651, 5'-TGCCCTCCTCTCTCAGCCATGATCG-3' and RK22652, 5'-TCGCTTGACACCACAGCAATAGC-3', at an annealing temperature of  $65^\circ\text{C}$ ; RK21651, 5'-AGGGCCAGCTCATTCTCCACTCA-3' and RK22651 at an annealing temperature of  $65^\circ\text{C}$ ; RK22649, 5'-ATCTCCAGGATCAGGTGGAAGCCG-3' and RK22650, 5'-TGGCTGGGTAGCGGTTTTTGC-3' at an annealing temperature of  $66^\circ\text{C}$ .

##### Protein Extraction

After sacrificing the mice in a  $\text{CO}_2$  chamber, the tissues were sampled for Coomassie-stained gels by extraction of the cytoskeletal, Triton X-100-insoluble fraction. Tissue was minced with a razor blade and resuspended in 200  $\mu$ l of extraction solution (20 mM Tris, pH 7.4, 0.6 M KCl, 1% Triton X-100, and 0.3 mg/ml fresh phenylmethylsulfonyl fluoride added before use). This was sonicated in a cup-horn sonicator at full power for  $2 \times 2$  min and spun in a microcentrifuge for 10 min at full speed. The supernatant was discarded, and the pellet was resuspended in 200  $\mu$ l of extraction solution. This was repeated twice, and the pellet was resuspended in 50  $\mu$ l of resuspension solution (9 M urea, 10 mM Tris, pH 8.0, and 10%  $\beta$ -mercaptoethanol) and stored at  $-70^\circ\text{C}$ .

For Western blotting, total protein was extracted by mincing tissue in 100  $\mu$ l of resuspension solution, sonication at full power in a cup-horn sonicator for  $2 \times 1$  min, and boiling for 5 min. The samples were centrifuged for 10 min at full speed in a microcentrifuge, and the pellet was discarded. The supernatant was stored at  $-70^\circ\text{C}$ .

##### SDS-PAGE Gels

For Western blots, 15% acrylamide SDS-PAGE gels were run according to Maniatis (16). Gels were run at 135 V for 72 h. For Coomassie Blue staining 12% gels were prepared using the LongRanger solution (FMC Bioproducts) according to the manufacturer's instructions. Gels were run at 175 V for 13 h.

##### Western Blots

Transfer of the protein from the gel onto Immobilon-P transfer membrane (Millipore) was achieved using a Multiphor II Nova Blot electrophoretic transfer apparatus (LKB). Transfers were performed in a

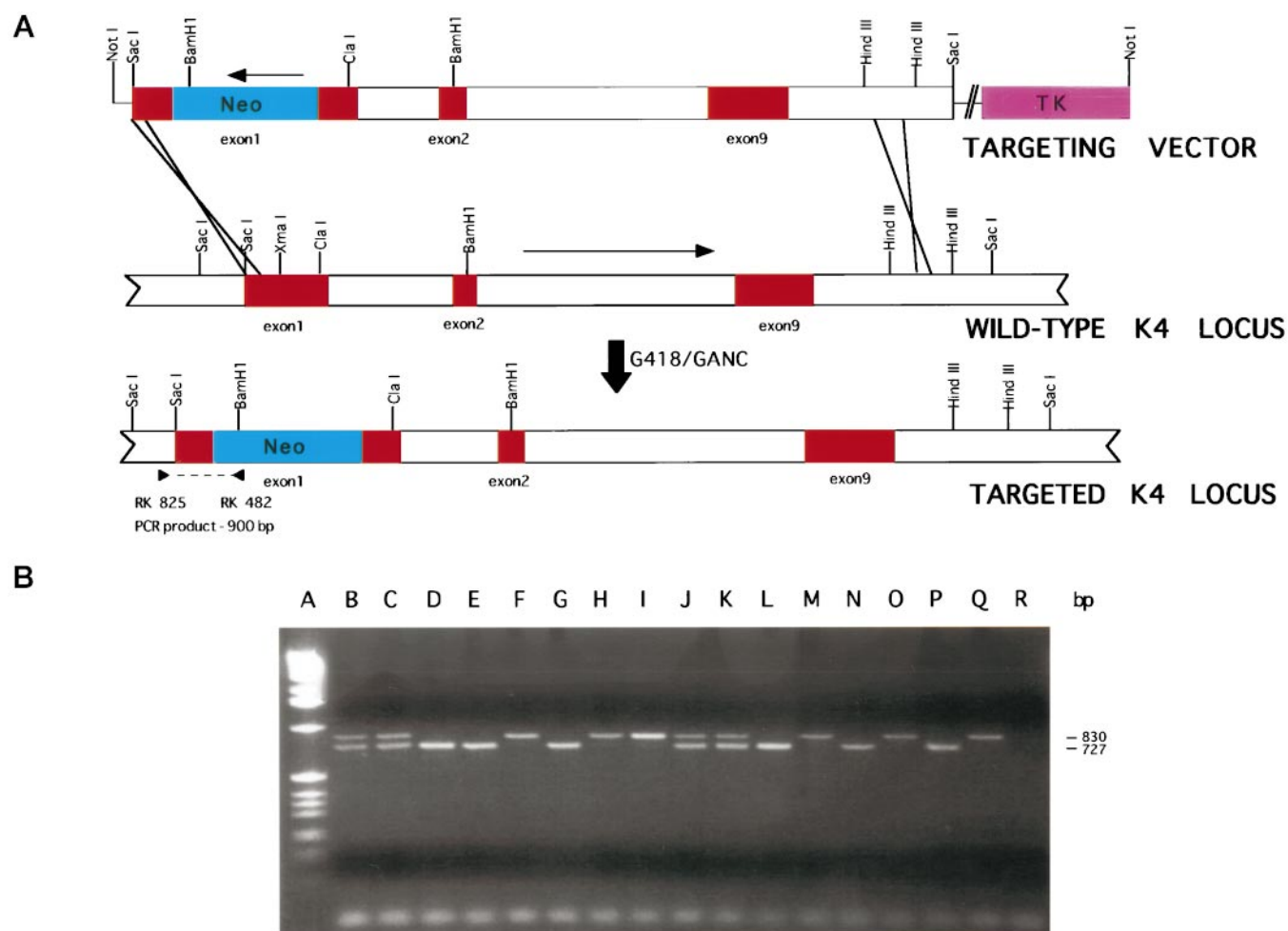


**FIG. 1. Targeting and genotyping of K4 knockout mice.** *A*, a schematic of the targeting vector and the successful homologous recombination event. Identified exons are in red, the neo cassette is in blue, and the TK cassette is in lavender. Some restriction sites are indicated. The arrows indicate the transcriptional orientations of the K4 gene and the neo cassette. The PCR reaction used to identify positive ES cells is shown. *B*, a 1% agarose gel stained with ethidium bromide showing the products of the PCR with three primers used to genotype the mice as described in the text. This is a representative sample of two litters. Lane A is a 1-kb ladder used as a marker. Lanes B–Q are from individual members of the two litters. Lane R is a negative control. The upper product is from the targeted allele and the lower is from the wild-type allele.

continuous transfer buffer of 39 mM glycine, 48 mM Tris, 0.0375% SDS, and 20% methanol for 1 h at a current of 0.8 mA/cm<sup>2</sup>. The membrane was blocked overnight at 4 °C with shaking in 0.1% Tween 20, 5% Blotto, and 10% sheep serum in 1× TBS. Two 10-min washes with 1× TBS-T were done. The membrane was then incubated in primary antibody diluted in 1× TBS-T and 5% Blotto for 2 h at room temperature. The membrane was washed twice as above and incubated with secondary antibody from the ECL kit diluted 1:5000 in TBS-T and 5% Blotto for 1 h at room temperature. Four washes in TBS-T were done before proceeding to develop the blot with the ECL immunodetection kit (Amersham Pharmacia Biotech) according to the manufacturer's instructions.

Antibodies used were as follows: 6B10, anti-human keratin 4 monoclonal antibody (Sigma) at 1:500 dilution; AE8, anti-human keratin 13 monoclonal antibody (ICN) at 1:250 dilution; AE1, anti-human type I keratin monoclonal antibody (ICN) at 1:200 dilution; and AE3, anti-human type II keratin monoclonal antibody (ICN) at 1:200 dilution. All are cross-reactive with their respective mouse keratins.

#### Histopathology

After sacrificing the mice by CO<sub>2</sub> asphyxiation, an autopsy was performed searching for gross abnormalities and sampling relevant organs by immersion fixation in 10% neutral buffered formalin. Paraffin-embedded tissue was sectioned at 4 μm and stained with hematoxylin-eosin for light-microscopy. To evaluate proliferating cells, 4-μm sections of formalin-fixed, paraffin-embedded tissue were subjected to PCNA-specific immunostaining employing a PCNA antibody (anti-human PCNA, cross-reacts with mouse, PharMingen, San Diego, CA; dilution 1/400) and the ABC kit according to the suggestions of the manufacturer (Vector Inc., Burlingame, CA). Pretreatment of the sec-

tions with heated citrate buffer (10 mM) was found to vastly enhance specific staining.

#### RESULTS

**Generating Mice Lacking K4 Expression**—The coding sequences of keratins share a high degree of homology. We isolated part of the mouse keratin 4 genomic sequence by generating degenerate PCR primers corresponding to sequences in exons 3 and 4. This pair of primers, designated RK567 and RK568, was used for amplification of products containing intron 3 of type II keratins from mouse genomic DNA. The PCR reaction yielded six products, one of which, pMK1, when cloned and sequenced at one end was found to have 61 bp, which had 100% identity to exon 4 of mouse keratin 4 (19). We isolated a 490-bp fragment from this clone that contained the unique sequences corresponding to intron 3 of K4 and used it to screen a genomic library from the strain 129/Ola. The screening yielded seven independent clones; the DNA from clone 3 was used to construct the targeting vector.

A 9.5-kb *SacI* fragment from clone 3 was subcloned and found to harbor the complete K4 gene. This clone, designated pK4-4, had a unique *XmaI* site at nucleotide position 519 corresponding to the 12th codon of the K4 gene. A 1.7-kb neomycin phosphotransferase gene expression cassette (PGK-neo) was introduced into the unique *XmaI* site to generate the

targeting vector, which also contained the PGK-tk gene for negative selection. Since the PGK-neo cassette was located at the 12th codon of the K4 gene, the modified locus was expected to result in a K4 gene null mutation.

Linearized DNA from the targeting vector (Fig. 1A) was introduced into the mouse embryonic stem (ES) cell line WW6 by electroporation and the cells were subjected to selection in G418 and ganciclovir (GANC). One hundred eleven discrete colonies were isolated and examined for the desired gene targeted events by PCR. The PCR primers RK482 and RK825 were expected to yield a 900-bp product from the DNA of appropriately modified cells only. Eight of the 111 clones gave the 900-bp product for a targeted efficiency of 7.2%. The GANC selection resulted in a less than 2-fold enrichment.

Cells from three of the eight clones containing the K4 gene modification, designated A5, A14, and B15, were injected into blastocysts from C57BL/6 (B6) mice. All three cell lines yielded chimeras, many of which had very high levels (>95%) of contribution from the ES cells as determined by coat color. Several of these chimeras transmitted the ES cell genome through their germ line when mated with B6 females. Heterozygous mice derived from clones A5 and A14 were interbred, and the offspring were genotyped at the K4 locus. We used a PCR amplification scheme with three PCR primers to identify the wild-type and mutant loci. Results of analysis of two representative litters are shown in Fig. 1B. The wild-type locus is represented by a 727-bp product and the mutant locus by an 830-bp product. The F2 offspring contained three classes of mice, and among a set of 156 F2 offspring tested, 37 were +/+, 80 were +/-, and 39 were -/-. These results indicate that the modified gene segregates in a Mendelian fashion and that mice that are homozygous for the null mutation are viable. Furthermore, the wild-type K4 gene does not seem to be critical for normal development.

**Absence of Expression of K4 in Mutant Mice**—We used three different approaches to examine the expression of K4 in mutant mice. To test the expression of the modified K4 locus at the RNA level, we used an RT-PCR. Three sets of primers were used for this purpose. The first set, RK22651 and RK22652, flank the neomycin phosphotransferase gene (neo) cassette insertion site in the K4 gene. They yield a 98-bp fragment from the wild-type (WT) transcript and a 1.8-kb fragment, unamplified in the conditions employed, from the chimeric RNA. The second set of primers, RK21651 and RK22651, uniquely amplify a 270-bp product only from the chimeric RNA containing the neo cassette and not from the normal transcript. The third set of primers, RK22649 and RK22650, amplify a 485-bp product from the normal as well as the chimeric transcript. RNA from total esophagi of wild-type and homozygous mutant mice was used as the substrate for RT-PCR. The results are shown in Fig. 2a. We were able to detect the expected 98-bp product with the primer set RK22651/RK22652 and the 485-bp product using primer set RK22649/RK22650 in RNA from wild-type mice. RNA from mutant mice yielded the 270-bp product with primer set RK21651/RK22651, and a small amount of the 485-bp product with the third primer set. These results show that the mutant mice indeed contained the gene modification and that the modified locus produces a chimeric transcript, although its steady state level might be low.

To further assess the status of expression of the modified locus, RNA from esophagi of +/+, +/-, and -/- mice was fractionated on agarose gels and Northern blots were hybridized with a probe obtained from amplification of genomic DNA using primers RK22649/RK22650. This 485-bp product contains 125 bp of the unique 3'-end of the coding region and much of the unique 3'-untranslated region of K4. Results of this

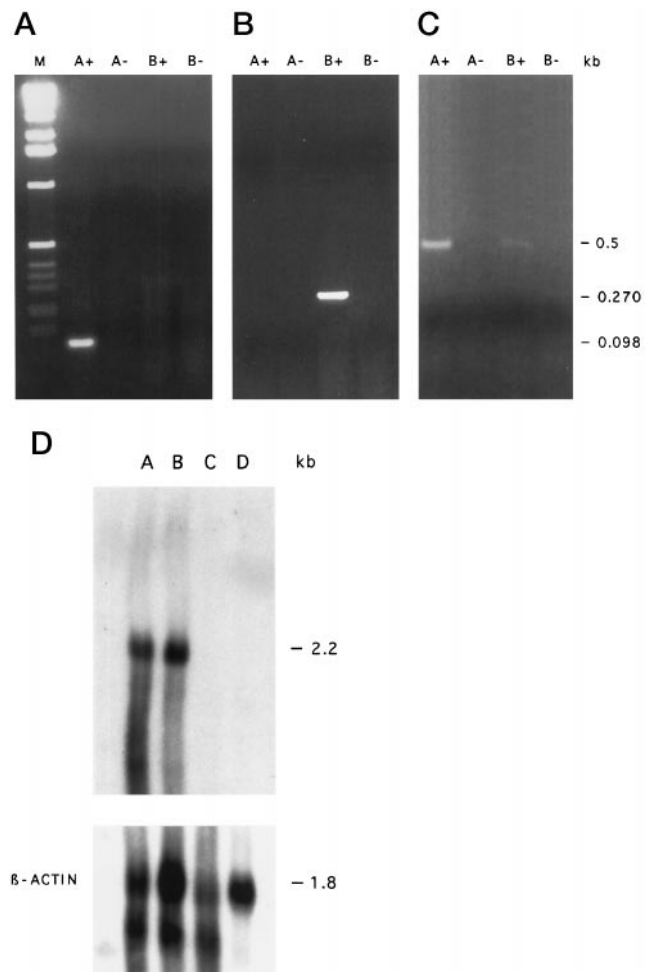
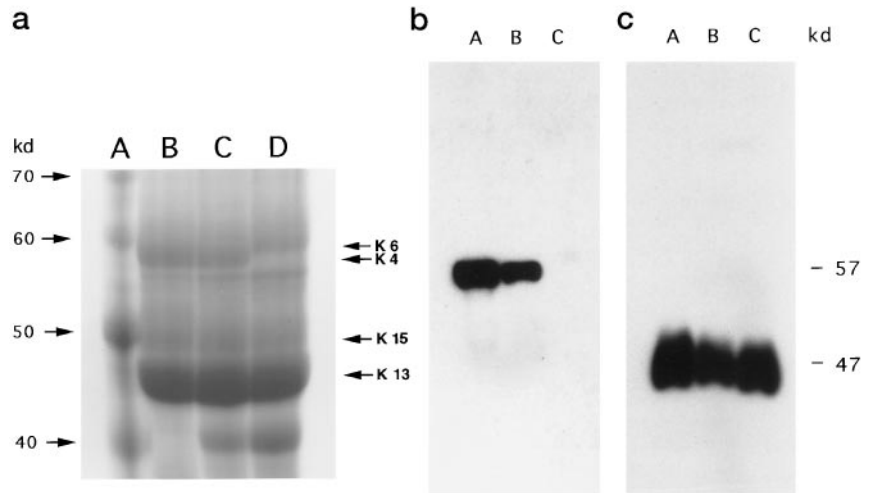


**FIG. 2. Studies of the expression of the K4 transcript in K4  $-/-$  animals and controls.** Panels A–C, a 1% agarose gel stained with ethidium bromide showing the products of RT PCR of mouse esophagus for K4 expression. RNA was extracted from 2-month-old mouse esophagus. In panel A, primers RK 22651 and RK 22652 surrounding the neo cassette were used. Lanes A, wild-type esophagus, with (+) and without (–) reverse transcriptase; lanes B, homozygous esophagus, with (+) and without (–) reverse transcriptase; Lane M, 1-kb marker. Only wild-type mice are expected to yield a product. In panel B, primers RK 21651 and RK 22651 were used to amplify across the 5' end of the neo cassette. Lanes A, wild-type esophagus, with (+) and without (–) reverse transcriptase; lanes B, homozygous esophagus, with (+) and without (–) reverse transcriptase. Only mutant transcripts are expected to yield a product. In panel C, primers RK 22649 and RK 22650 in exon 9 were used. Lanes A, wild-type esophagus, with (+) and without (–) reverse transcriptase; lanes B, homozygous esophagus, with (+) and without (–) reverse transcriptase. Both wild-type and mutant transcripts are expected to yield a product. In panel D, Northern blot of esophageal RNA with pMK4–3' probe and  $\beta$ -Actin control. RNA was extracted from 2-month-old mouse esophagus. Lanes A, wild-type esophagus; lanes B, heterozygous esophagus; lane C, homozygous esophagus; lane D, wild-type liver. The  $\beta$ -actin probe hybridizes to two transcripts in muscle.

experiment are shown in Fig. 2b. RNA from +/+ and +/- mice yielded the expected 2.25-kb product, while no transcript was detected in -/- mice. Taken together, the RNA analysis shows that the K4 -/- mice do not produce a transcript from which a full-length K4 protein could be synthesized.

**K4  $-/-$  Mice Do Not Produce the K4 Protein**—We attempted to detect the K4 protein by two different methods. In the first method, a keratin-enriched fraction from total protein extracts prepared from esophagi was fractionated on polyacrylamide gels and the different keratins were visualized by Coomassie Blue staining. Results of this experiment are shown in Fig. 3a. K4 is a 57-kDa protein and is detectable in extracts from +/-

**FIG. 3. Studies of Keratin proteins in K4  $-/-$  animals and controls.** In panel a, Coomassie Blue-stained SDS-PAGE gel of esophageal keratin extracts. Protein was extracted from 2-month-old mouse esophagus. Lanes A, 10-kDa marker; B, wild-type mouse; C, heterozygous mouse; D, homozygous mouse. Note the increase in a 59-kDa protein, consistent in mass with MK6, in  $k4^{-/-}$  mice and the presence of an unidentified 40-kDa protein. In panels b and c, Western blots of total protein extracts from two month old mouse esophagus. Panel b, antibody 6B10 against human K4 was used. Lanes A, wild-type mouse; B, heterozygous mouse; C, homozygous mouse. Panel c, antibody AE8 against human K13 was used. Lanes A, wild-type mouse; B, heterozygous mouse; C, homozygous mouse.



mice, and in  $+/-$  mice at somewhat reduced levels. No K4 protein was detectable in extracts from  $-/-$  mice. The levels of K13, the partner for K4, were identical in all three groups of mice. This analysis also revealed two other interesting features. Although not quantitative, we observed increased levels of a protein at 59 kDa, consistent in molecular mass with mouse keratin 6, in  $K4^{-/-}$  mice. K6 is known to be expressed suprabasally in some internal stratified epithelia, and there are some reports of its expression in human esophagus (20–22). Another protein with a molecular mass of 40 kDa, consistent with a type I keratin, although not present in WT mice, was present in  $+/-$  and  $-/-$  mouse extracts. The identities of these proteins remain to be definitively elucidated.

In a second assay, total protein extracts from the three groups of mice were fractionated and Western blot analysis was conducted with specific antibodies against K4 and K13. Results of this experiment are shown in Fig. 3 (b and c). Extracts from mice from all three groups contained K13, while the K4 antibodies detected the protein only in  $+/+$  and  $+/-$  mice. These results unambiguously show that the genetic modification introduced into the K4 gene results in a null mutation.

In addition, Western blots were performed using the antibodies AE1, which reacts with many type I keratins, and AE3, which reacts with all known type II keratins (data not shown). Blotting with AE3 confirmed the absence of MK4 in  $K4^{-/-}$  mice and the identity of the protein at 59 kDa as a type II keratin. The protein at 40 kDa was not detected by either AE1 or AE3.

***K4  $-/-$  Mice Exhibit Phenotypic Abnormalities of Multiple Epithelial Tissues***—The fact that the mutant allele segregates in a Mendelian fashion suggested that K4 is not necessary for normal development. We followed the mice for up to 2 years and the homozygotes were indistinguishable from their  $+/+$  and  $+/-$  littermates, by visual inspection. Since the expression of K4 is restricted to internal epithelia, we sampled a number of different tissues where K4 is known to be expressed and examined them by histological methods. The tissues that were sampled included skin, buccal mucosa, gum/teeth, tongue, esophagus, forestomach, glandular stomach, colon/rectum, lung, genitourinary tract, and the cornea. All these tissues, except the skin, are known to express K4. We observed histologic changes in tongue, esophagus, forestomach, cornea, and the skin.

Results of histological analysis of the esophagus are shown in Fig. 4 (a–d). Changes in the esophagus were observed as early as 2 months (Fig. 4, a and b) in the  $-/-$  mice, including hyperplasia and nuclear atypia in the basal epithelial layer. The nuclear atypia consisted of enlarged nuclei and nucleoli with clumped chromatin. In the suprabasal layers, increased

nuclear atypia and altered nuclear morphology were evident. The suprabasal cells also had a characteristic clear area around the nucleus, designated the “cell within a cell” appearance. Overall, the epithelium was thickened and cells appeared to be immature, with fewer differentiated cells, diminished keratohyalin granules, and a disturbance in the maturation of cell layers. The epithelium also exhibited parakeratosis and dyskeratosis with a diffuse and disorganized keratin layer. We also observed bacterial invasion and hemorrhagic exudate in the lumen and infiltration of the subepithelial space and the basal layer with neutrophils. In 5-month-old  $-/-$  mice (Fig. 4, c and d), the keratin layer became more disorganized and we observed progression of all other changes noted in the 2-month-old mice. The heterozygous mice, even at 7 months of age, did not show any of the changes and were histologically indistinguishable from their WT littermates. In contrast, the forestomach of 2- and 5-month-old  $-/-$  mice had increased cellularity of the basal layer but no dysplasia was detected (results not shown).

The corneal epithelium was abnormal in 2-month-old  $-/-$  mice (Fig. 4, e and f). There was increased thickness compared with WT mice. Basal cell hyperplasia was evident. The nuclear morphology in all layers was altered, and the “cell within a cell” appearance was a common feature. The results of histological analysis of the tongue are shown in Fig. 5 (a and b). At 2 months, the tongue from  $-/-$  mice did not show any significant changes. Significant differences were observed in 5-month-old  $-/-$  mice. At this age, the dorsal surface was normal. However, the ventral surface revealed cellular hyperplasia and parakeratosis. There were also interdigitations or pegs of epithelium into the submucosa such as those normally found only in the dorsal surface.

It is of interest to note that we observed some differences in the skin of  $-/-$  mice (Fig. 5, c and d). We observed an age-dependent increase in the deposition of melanin throughout the dermis. No melanin deposition was observed in the dermis of  $+/+$  or  $+/-$  mice.

***K4  $-/-$  Mice Exhibit Abnormal Epithelial Proliferation as Measured by PCNA Staining***—Some of the changes that were observed in  $K4^{-/-}$  mice suggested that the absence of K4 leads to hyperplasia. We tested this feature by staining tissue sections for PCNA, which is an indicator of cell proliferation. Esophagi from  $K4^{+/+}$  mice showed proliferation only in the basal layer with occasional staining of isolated cells in the suprabasal layers. In  $K4^{-/-}$  mice, proliferating cells were detected throughout the epithelium (Fig. 5, e and f). Similar features were also observed in the tongue (data not shown).

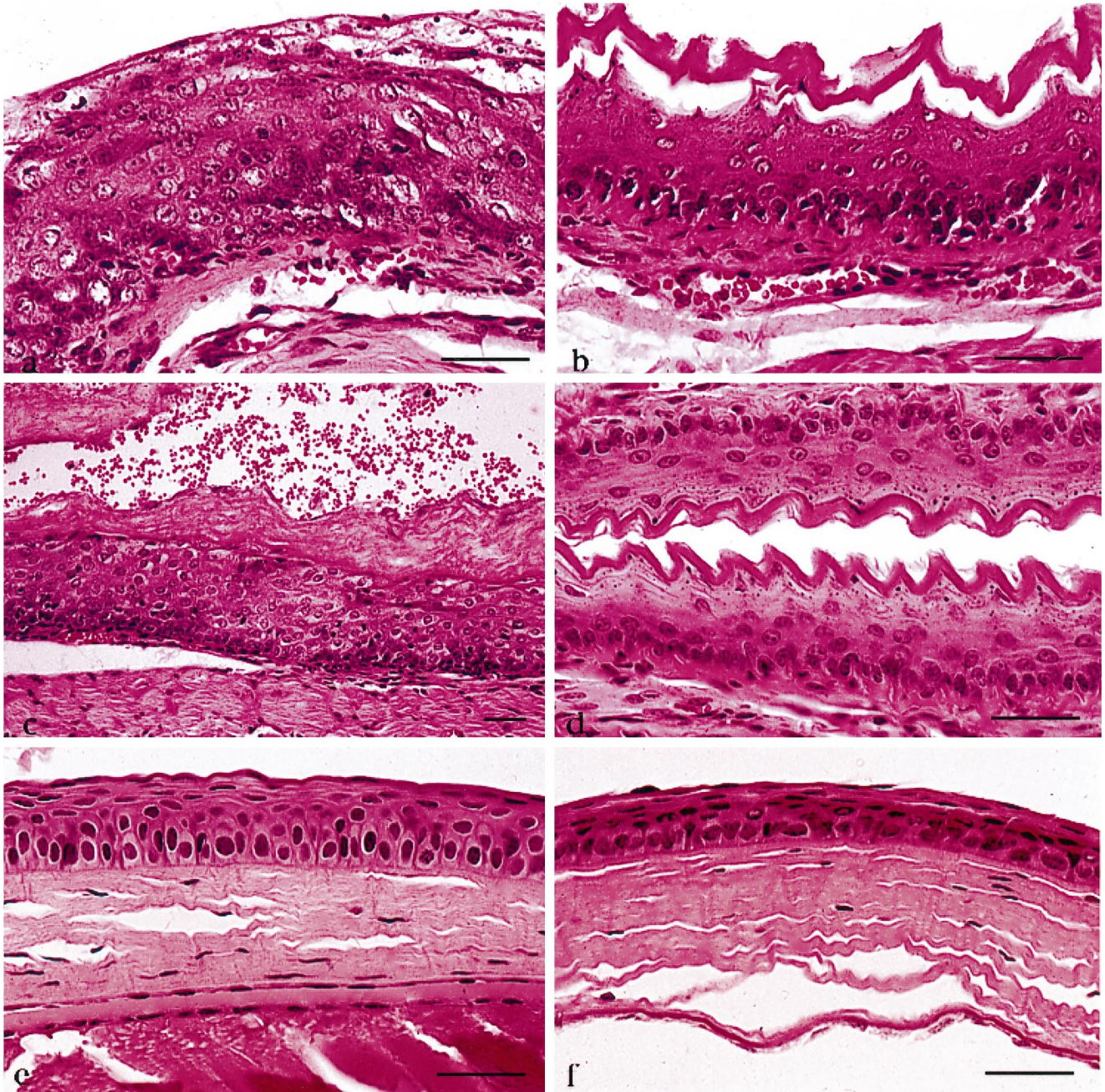


**FIG. 4. Histopathology of epithelia in K4  $-/-$  and WT littermate control mice.** Micrographs of K4  $-/-$  tissues are shown on the left, WT littermate controls on the right. All tissues were formalin-fixed, paraffin-embedded, cut at 4  $\mu\text{m}$ , and stained with hematoxylin-eosin. The scale bar represents 20  $\mu\text{m}$ . *a*, K4  $-/-$ , 2 months of age, esophagus. Note the disturbed architecture and hyperplasia of the epithelium. *b*, K4  $+/+$ , 2 months of age, esophagus. Regular appearance of the esophagus. *c*, K4  $-/-$ , 5 months of age, esophagus. Changes are apparent as in *a*, but more pronounced. Note the increased epithelial thickness and hemorrhagic exudate in the lumen. *d*, K4  $+/+$ , 5 months of age, esophagus. Regular appearance. *e*, K4  $-/-$ , 5 months of age, cornea. Note hyperplasia and immaturity of the epithelial layers. *f*, K4  $+/+$ , 5 months of age, cornea. Regular epithelial appearance.

#### DISCUSSION

We generated mice with a modification in the K4 gene. There are several lines of evidence which support the view that these mice contain a null mutation in the K4 gene. The gene modification construct was prepared by insertion of a selectable gene cassette at a position that corresponds to codon 12 of the normal gene product. Since the gene cassette is in the opposite transcriptional orientation to that of K4, the insertion site contains several stop codons in all reading frames. PCR as well as Southern blot analysis showed that the ES cells contained the correct targeted event. Northern blot analysis revealed that esophagi from  $-/-$  mice did not contain a detectable message

corresponding to the K4 probe. The most convincing evidence that the K4  $-/-$  mice did not produce K4 protein was obtained from examination of keratin-enriched protein fractions and by Western blot analysis using K4-specific antibodies.

K4 and K13 form heterodimers in normal epithelial cells. Western blot analysis with anti-K4 and K13 human antibodies revealed that K4  $-/-$  mice did not contain any detectable K4 protein, while K13 levels remained unchanged. Previous work showed that, when one member of a pair of keratins is absent, its natural partner tends to get degraded (23–25). The fact that K13 levels remain unaltered in K4  $-/-$  mice suggests that the regulation of members of the K4 and K13 pair may be different

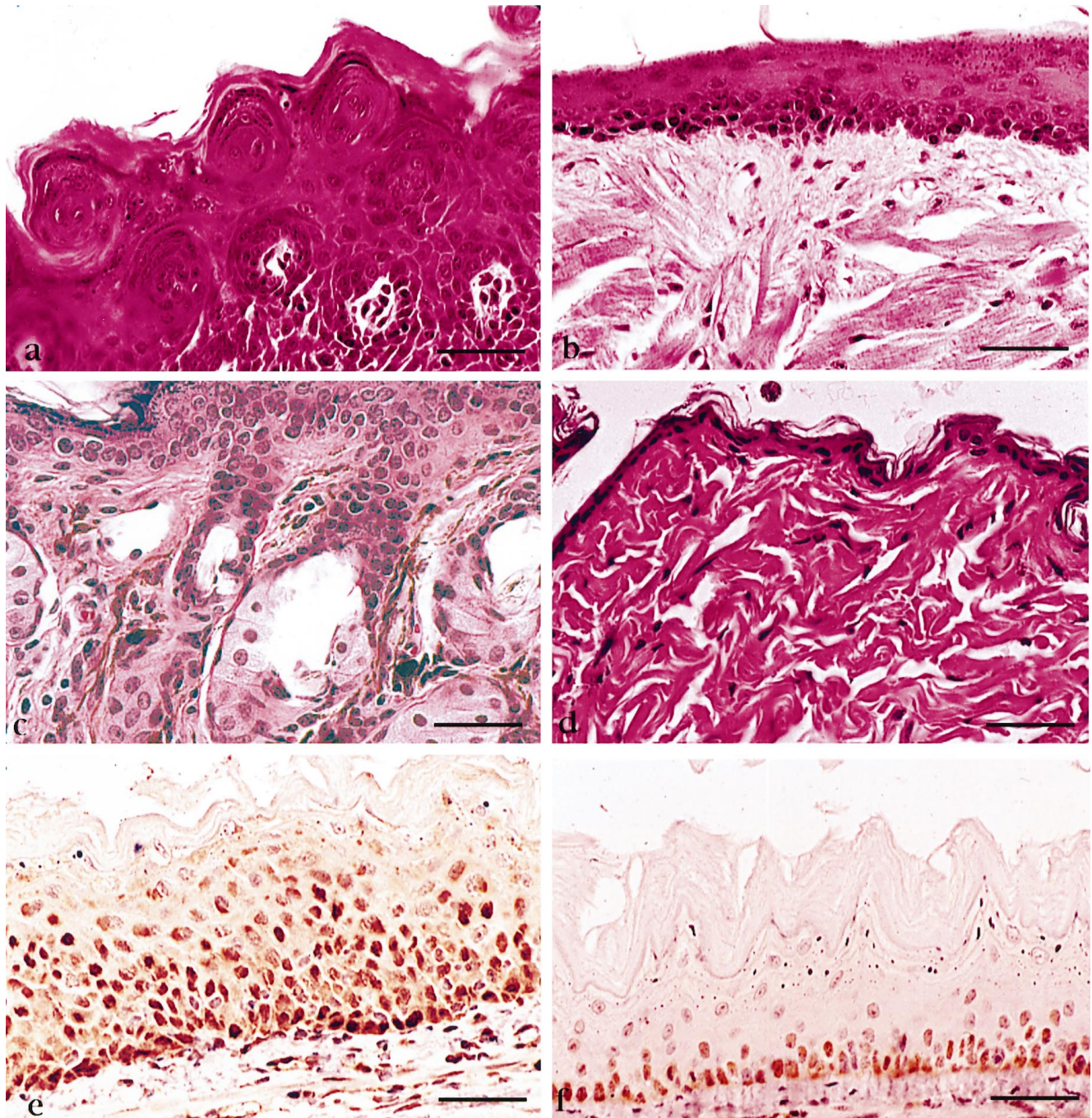


**FIG. 5. Additional histopathology of epithelia in K4  $-/-$  and WT littermate control mice.** Micrographs of K4  $-/-$  tissues are shown on the left, WT littermate controls on the right. All tissues were formalin-fixed, paraffin-embedded, cut at 4  $\mu$ m, and stained with hematoxylin-eosin (a-d) or specifically for PCNA by immunohistochemistry (e and f). The scale bar represents 20  $\mu$ m. a, K4  $-/-$ , 5 months of age, ventral tongue. This micrograph shows a strikingly different epithelial architecture. b, K4  $+/+$ , 5 months of age, ventral tongue. Regular appearance. c, K4  $-/-$ , 5 months of age, skin. Note the subcutaneous melanin deposits. d, K4  $+/+$ , 5 months of age, skin. Regular appearance and absence of subcutaneous melanin. e, K4  $-/-$ , 5 months of age, esophagus, anti-PCNA immunohistochemistry. Note the presence of PCNA+ cells in all epithelial layers. f, K4  $+/+$ , 5 months of age, esophagus, staining as in e, PCNA+ cells are only present in the basal epithelial layer.

from that of other keratins. Alternatively, K13 may be capable of pairing with another member of the keratin family when K4 is absent.

One candidate for this pairing may be the protein at 59 kDa visible in the Coomassie-stained gel. This protein is present in the keratin-enriched extract, is consistent in molecular mass with mouse keratin 6, and is detected by AE3 as a type II keratin. Unfortunately, we were unable to obtain anti-K6 antibody, and definitive identification of this protein awaits the public availability of such antibody.

Although the protein at 40 kDa is present in a keratin-

enriched extract and is similar in size to several type I keratins, it was not detected by either AE1 or AE3. AE1 is known not to detect several type I keratins, notably 9, 11, 12, 13, 17, and 18, so we have not ruled out the identification of this protein as a keratin. Definitive identification will likely require peptide sequencing.

K4 does not appear to be required for normal growth and development, and K4-deficient mice do not show any gross phenotypic differences as compared with their WT and heterozygote littermates. The K4  $-/-$  mice have normal lifespans and breed normally. They do show a spectrum of changes in

internal tissues where K4 is normally expressed. The most striking feature of K4  $-/-$  mice is that esophageal epithelial cells do not terminally differentiate but have abnormal proliferation. These characteristics are reminiscent of dysplastic changes in the esophagus of transgenic mice with cyclin D1 overexpression (26).

The hyperproliferative phenotype associated with K4 deficiency in mice is very similar to what has been observed in K1 deficiency. K1 deficiency in humans leads to epidermolytic hyperkeratosis (11–13). K4 deficiency, as in K1 deficiency, leads to basal cell hyperplasia, a “cell within a cell” appearance, abnormal nuclei, reduced keratohyalin granules, disruption of the keratin layer, and an inflammatory response. K4 and K1 have analogous functions, as both are expressed in the suprabasal layers of stratified epithelia. Despite the similarities between the K1 and K4 deficiencies, the K1 deficiency leads to skin blistering, and no such blistering of the esophagi or oral mucosa was observed in the K4  $-/-$  mice. These differences might reflect the greater stresses that the skin is subjected to relative to internal epithelia. We also observed increased bacterial presence, a hemorrhagic exudate, and an inflammatory response in the esophagus of K4  $-/-$  mice, suggesting that the keratin layer may provide protective functions against microbial agents.

As keratin 4 is not found in adult skin, we did not predict phenotypic changes in that tissue. Therefore, the findings of higher levels of melanin deposition with increased melanocytes in the dermis were surprising. In normal mouse tissue, melanocytes are found predominantly in hair follicles and melanin is deposited in hair (27). K4 expression was found in the periderm of 16-day-old mouse embryos (28). No data were available at other times in embryonic development, and there are no reports of K4 in hair follicles. In humans, K4 is present in all layers of the epidermis at 10 weeks and gradually disappears, starting from the basal layers at 15 weeks and becoming totally absent at around 20 weeks (20). This period corresponds to the early fetal period when melanoblasts derived from the neural crest migrate through the dermis into the basal layer of the epidermis (29). The role of K4 in melanocyte migration or melanin deposition needs further investigation.

WSN (OMIM 193900) is a benign autosomal dominant disorder characterized by thickened, white opalescent spongy-fold mucosa primarily in the mouth but also in the vaginal, rectal, and esophageal epithelia. The lesions show hyperplasia, “cell within a cell” appearance, lack of cellular maturation, keratin filament clumping, and mild inflammation (33–37). Mutations in K4 and K13 were found to be the cause of WSN (14, 15). Patients with WSN show variable phenotypes, and the lesions are generally focal in nature. The phenotypic spectrum observed in K4  $-/-$  mice is similar, but not identical to that seen in WSN patients. In the mice, there are no changes in the buccal mucosa and the epithelial hyperplasia is generally not as extreme as it is in WSN. The differences may reflect the genetic heterogeneity of humans, slightly different patterns of gene expression, or the nature of the mutations, which in WSN act in a dominant-negative fashion as opposed to the recessive nature of the modified mouse K4 locus.

We observed that the corneal epithelium in K4-deficient mice shows basal cell hyperplasia. As K4 is known to be expressed in human cornea (30–32), it is possible that null mutations in K4 would lead to a corneal phenotype in humans. Hereditary benign intraepithelial dyskeratosis (OMIM 127600) is an autosomal dominant disorder with a histological appearance identical to that of WSN. It differs from WSN in the absence of changes

in the esophagus of patients and in the presence of corneal hyperkeratosis. Based on the similarities in the corneal phenotypes of K4-deficient mice and patients with hereditary benign intraepithelial dyskeratosis, we suggest that K4 or K13 mutations may be responsible for this disorder.

**Acknowledgments**—We acknowledge the assistance of Harry Hou (Albert Einstein College of Medicine) for blastocyst injections, Jorge E. Bermudez (Rockefeller University) for skilled technical assistance, Annegret Muller (Massachusetts General) for PCNA staining, and Elaine Fuchs and Elizabeth Hutton (University of Chicago) for reagents and advice.

## REFERENCES

- Fuchs, E., and Weber, K. (1994) *Annu. Rev. Biochem.* **63**, 345–382
- Compton, J. G., Ferrara, D. M., Yu, D. W., Recca, V., Freedberg, I. M., and Bertolino, A. P. (1991) *Ann. N. Y. Acad. Sci.* **642**, 32–43
- Steinert, P. M., and Roop, D. R. (1988) *Annu. Rev. Biochem.* **57**, 593–625
- Moll, R., Franke, W. W., Schiller, D. L., Geiger, B., and Krepler, R. (1982) *Cell* **31**, 11–24
- Klymkowsky, M. W., Miller, R. H., and Lane, E. B. (1983) *J. Cell Biol.* **96**, 494–509
- Bonifas, J. M., Rothman, A. L., and Epstein, E., Jr. (1991) *Science* **254**, 1202–1205
- Coulombe, P. A., Hutton, M. E., Letai, A., Hebert, A., Paller, A. S., and Fuchs, E. (1991) *Cell* **66**, 1301–1311
- Lane, E. B., Rugg, E. L., Navsaria, H., Leigh, I. M., Heagerty, A. H., Ishida-Yamamoto, A., and Eady, R. A. (1992) *Nature* **356**, 244–246
- Chan, Y., Anton-Lamprecht, I., Yu, Q. C., Jackel, A., Zabel, B., Ernst, J. P., and Fuchs, E. (1994) *Genes Dev.* **8**, 2574–2587
- Rugg, E. L., McLean, W. H., Lane, E. B., Pitera, R., McMillan, J. R., Dopping-Hepenstal, P. J., Navsaria, H. A., Leigh, I. M., and Eady, R. A. (1994) *Genes Dev.* **8**, 2563–2573
- Cheng, J., Syder, A. J., Yu, Q. C., Letai, A., Paller, A. S., and Fuchs, E. (1992) *Cell* **70**, 811–819
- Chipev, C. C., Korge, B. P., Markova, N., Bale, S. J., DiGiovanna, J. J., Compton, J. G., and Steinert, P. M. (1992) *Cell* **70**, 821–828
- Rothnagel, J. A., Dominey, A. M., Dempsey, L. D., Longley, M. A., Greenhalgh, D. A., Gagne, T. A., Huber, M., Frenk, E., Hohl, D., and Roop, D. R. (1992) *Science* **257**, 1128–1130
- Richard, G., De Laurenzi, V., Didona, B., Bale, S., and Compton, J. (1995) *Nat. Genet.* **11**, 453–455
- Rugg, E., McLean, W., Allison, W., Lunny, D., Macleod, R., Felix, D., Lane, E., and Munro, C. (1995) *Nat. Genet.* **11**, 450–452
- Sambrook, J., Fritsch, E. F., and Maniatis, T. (1989) *Molecular Cloning: A Laboratory Manual*, 2nd Ed., Cold Spring Harbor Laboratory, Cold Spring Harbor, NY
- Wurst, W., and Joyner, A. L. (1995) in *Gene Targeting: A Practical Approach* (Joyner, A. L., ed) 1st Ed., p. 234, Oxford University Press, Oxford
- Laird, P. W., Zijderveld, A., Linders, K., Rudnicki, M. A., Jaenisch, R., and Berns, A. (1991) *Nucleic Acids Res.* **19**, 4293
- Knapp, B., Rentrop, M., Schweizer, J., and Winter, H. (1986) *Nucleic Acids Res.* **14**, 751–763
- Moll, R., Moll, I., and Wiest, W. (1982) *Differentiation* **23**, 170–178
- Sawaf, M. H., Ouhayoun, J. P., Shabana, A. H., and Forest, N. (1992) *Pathol. Biol.* **40**, 655–665
- Viaene, A. I., and Baert, J. H. (1995) *Anat. Rec.* **241**, 88–98
- Kulesh, D. A., and Oshima, R. G. (1988) *Mol. Cell. Biol.* **8**, 1540–1550
- Lersch, R., Stellmach, V., Stocks, C., Giudice, G., and Fuchs, E. (1989) *Mol. Cell. Biol.* **9**, 3685–3697
- Lloyd, C., Yu, Q. C., Cheng, J., Turksen, K., Degenstein, L., Hutton, E., and Fuchs, E. (1995) *J. Cell Biol.* **129**, 1329–1344
- Nakagawa, H., Wang, T., Zuckerberg, L., Odze, R., Togawa, K., May, G., Wilson, J., and Rustgi, A. (1997) *Oncogene* **14**, 1185–1190
- Wolfe, H. G., and Coleman, D. L. (1966) in *Biology of the Laboratory Mouse* (Green, E. L., ed) 2nd Ed., McGraw-Hill Book Co., New York
- Nischt, R., Roop, D. R., Mehrel, T., Yuspa, S. H., Rentrop, M., Winter, H., and Schweizer, J. (1988) *Mol. Carcinogen.* **1**, 96–108
- Moore, K. L. (1988) *The Developing Human*, 4th Ed., W. B. Saunders Co., Philadelphia
- Lauweryns, B., van den Oord, J. J., De Vos, R., and Missotten, L. (1993) *Invest. Ophthalmol. Vis. Sci.* **34**, 1983–1990
- Wiley, L., SundarRaj, N., Sun, T. T., and Thoft, R. A. (1991) *Invest. Ophthalmol. Vis. Sci.* **32**, 594–602
- Van Muijen, G. N., Ruiter, D. J., Franke, W. W., Achtstatter, T., Haasnoot, W. H., Ponc, M., and Warnaar, S. O. (1986) *Exp. Cell Res.* **162**, 97–113
- Krajewska, I. A., Moore, L., and Brown, J. H. (1992) *Pathology* **24**, 112–115
- Frithiof, L., and Banoczy, J. (1976) *Oral Surg. Oral Med. Oral Pathol.* **41**, 607–622
- McGininis, J., Jr., and Turner, J. E. (1975) *Oral Surg. Oral Med. Oral Pathol.* **40**, 644–651
- Morris, R., Gansler, T. S., Rudisill, M. T., and Neville, B. (1988) *Acta Cytol.* **32**, 357–361
- Sayag, J., Jancovici, E., and Lacroix, J. (1985) *Ann. Dermatol. Venereol.* **112**, 759–760